A Matérn-Based Multivariate Gaussian Random Process for a Consistent Model of the Horizontal Wind Components and Related Variables

RÜDIGER HEWER, PETRA FRIEDERICHS, AND ANDREAS HENSE

Meteorological Institute, University of Bonn, Bonn, Germany

MARTIN SCHLATHER

School of Business Informatics and Mathematics, University of Mannheim, Mannheim, Germany

(Manuscript received 22 December 2016, in final form 24 August 2017)

ABSTRACT

The integration of physical relationships into stochastic models is of major interest, for example, in data assimilation. Here, a multivariate Gaussian random field formulation is introduced that represents the differential relations of the two-dimensional wind field and related variables such as the streamfunction, velocity potential, vorticity, and divergence. The covariance model is based on a flexible bivariate Matérn covariance function for the streamfunction and velocity potential. It allows for different variances in the potentials, nonzero correlations between them, anisotropy, and a flexible smoothness parameter. The joint covariance function of the related variables is derived analytically. Further, it is shown that a consistent model with nonzero correlations between the potentials and positive definite covariance function is possible. The statistical model is fitted to forecasts of the horizontal wind fields of a mesoscale numerical weather prediction system. Parameter uncertainty is assessed by a parametric bootstrap method. The estimates reveal only physically negligible correlations between the potentials.

1. Introduction

An appropriate representation of the covariance structure in spatial models of meteorological variables is essential when analyzing (Gandin 1965, 21–121; Kalnay 2003) meteorological data using data assimilation (Hollingsworth and Lönnberg 1986; Evensen 1994; Bonavita et al. 2012; Pu et al. 2016). This generally requires an appropriate representation of the background error covariance matrix. Further, spatial stochastic models for meteorological variables should respect physical relationships.

One of the first approaches to include physical consistency via differential relations between variables can be found in Kolmogorov (1941). Thiébaux (1977) introduced a covariance model for wind fields assuming geostrophic balance, thereby incorporating anisotropy in the geopotential height. Daley (1985) derived a covariance model for the horizontal wind components assuming a Gaussian covariance model for the velocity potential and the streamfunction, where he derived the differential relations between the potentials and the wind field. The covariance model proposed by Daley (1985) is rather flexible as it allows for geostrophic coupling, nonzero correlation of the streamfunction and velocity potential, and differing scales for the two potentials. Daley (1985) also considered geopotential height as an additional model variable. However, the resulting covariance function for the wind fields is not positive definite for many parameter combinations. Hollingsworth and Lönnberg (1986) adapted Daley's method and formulated a covariance function for the potentials using cylindrical harmonics. They show that on the synoptic scale the correlation between the potentials is small, such that Daley (1991) reformulated his model for zero correlations. These approaches (Thiébaux 1977; Hollingsworth and Lönnberg 1986; Daley 1985) as well as our model differ from current data assimilation methods, as they provide an explicit, parametric, and analytic covariance model for the

Denotes content that is immediately available upon publication as open access.

Corresponding author: Rüdiger Hewer, rhewer@uni-bonn.de

DOI: 10.1175/JAS-D-16-0369.1

background error. So-called control variable transform methods (Bannister 2008) describe the background error matrix in an implicit nonparametric way via its square root[1] using latent variables that model the physical variables. Sample-based methods like the ensemble Kalman filter (Evensen 1994) describe the error statistics based on estimates obtained from an ensemble.

The data assimilation literature (e.g., Thiébaux 1977; Hollingsworth and Lönnberg 1986; Daley 1985) typically uses the stochastic models in order to describe the covariance matrix of the background error, which is the difference of a forecast and the true field. Similar methods have also been used in order to describe the full turbulent field (Frehlich et al. 2001). There has also been considerable interest in describing the statistics of the velocity field directly or via its spectrum (Bühler et al. 2014; Lindborg 2015; Bierdel et al. 2016).

While Thiébaux (1977), Hollingsworth and Lönnberg (1986), and Daley (1985) include physical relations via differentiation of the covariance function, finite difference operators are used in Bayesian hierarchical models. For example, Royle et al. (1999) modeled the geostrophic relation of the pressure and wind fields.

In this paper, we propose a multivariate Gaussian random field (GRF) formulation for six atmospheric variables in a horizontal two-dimensional Cartesian space. Assuming a bivariate Matérn covariance for a streamfunction ψ and velocity potential χ, we derive the covariance structure of the horizontal wind components $\mathbf{U} = (u, v)^{\mathrm{T}}$, as well as vorticity $\nabla \times \mathbf{U} := -(\partial/\partial \mathbf{e}_2)u + (\partial/\partial \mathbf{e}_1)v$ and divergence $\nabla \cdot \mathbf{U}$. All of these quantities are connected via the Helmholtz decomposition, which states that for any given wind field $\mathbf{U}$ there exists a streamfunction ψ and velocity potential χ, such that $\mathbf{U} = \nabla \times \psi + \nabla\chi$, where $\nabla \times \psi := [-(\partial/\partial \mathbf{e}_2)\psi, (\partial/\partial \mathbf{e}_1)\psi]^{\mathrm{T}}$. In two dimensions and with appropriate boundary conditions this decomposition is unique. The curl and divergence of the wind field are given as $\nabla \times \mathbf{U} = \Delta\psi$ and $\nabla \cdot \mathbf{U} = \Delta\chi$, respectively, where Δ is the two-dimensional Laplace operator.

Our multivariate GRF formulation is novel for several reasons. While, for example, Daley (1985) only used the potentials to derive the covariance function of the wind fields, our model is formulated for all related variables, including a formulation for the potential functions and the wind field, as well as vorticity and divergence. Second, our model provides a formulation for anisotropy in the wind field and the related potentials. Further, we allow for nonzero correlations between the rotational and divergent wind components, which might be particularly relevant for atmospheric fields on subgeostrophic scales. We show that the scale parameters considered by Daley (1985) are inconsistent with nonzero correlations between the streamfunction and velocity potential, as they do not lead to a positive definite model. An exact derivation of the condition under which the covariance function of Daley's model is positive definite is given in appendix A. Further our model is a counterexample to a theorem of Obukhov (1954), which claims that there is no isotropic wind field with nonzero correlation of the rotational and nonrotational components of the wind field. More details to Obukhov's claim are given in appendix B.

The covariance function of our multivariate GRF will be incorporated into an upcoming version of the spatial statistics R package RandomFields (Schlather et al. 2016). This opens the possibility for a wealth of applications in spatial statistics, including the conditional simulation of the streamfunction and vector potential given an observed wind field, a consistent formulation of the covariance structure for both the potentials and the horizontal wind components to be used in data assimilation, or stochastic interpolation (kriging) of each of the involved variables given the others. Kriging is the process of computing the conditional expectation of a certain variable given others. It is typically used to interpolate fields.

To exemplify the multivariate GRF, we estimated its parameters for atmospheric fields of the numerical ensemble weather prediction system, COSMO-DE-EPS (Gebhardt et al. 2011), provided by the German Meteorological Service (DWD). COSMO-DE is a high-resolution forecast system that provides forecasts on the atmospheric mesoscale (Baldauf et al. 2011). Estimation is realized using the maximum likelihood method, while uncertainty in the parameter estimation is assessed by parametric bootstrap (Efron and Tibshirani 1994). We also discuss the meteorological relevance of the parameters.

The remainder of the paper is organized as follows. In section 2 we introduce the multivariate GRF and demonstrate how the physical relations and anisotropy are included in the model formulation. Section 3 introduces the COSMO-DE-EPS data. Section 4 is devoted to the parameter estimation and the assessment of the uncertainties, while section 5 presents and interprets the results of the estimation. We conclude in section 6 and discuss potential applications, limits, and extensions of our multivariate GRF.

2. Theory

An important aspect of our multivariate GRF is the inclusion of the differential relations between the

[1] For example, Cholesky decomposition.

atmospheric variables. Under weak regularity assumptions the derivative of a Gaussian process is again a Gaussian process (Adler and Taylor 2007). Hence, the assumption of Gaussianity of the streamfunction and the velocity potentials implies Gaussianity of all the considered variables. A zero-mean Gaussian process is uniquely characterized by the covariance function; we only need to study the joint covariance of a random field and its derivatives. A Gaussian process $X_{\mathbf{s}}$, $\mathbf{s} \in \mathbb{R}^d$ is a continuously indexed stochastic process. For each finite number of locations $\mathbf{s}_i$, $i = 1, \ldots, n$ the variables $X_{\mathbf{s}_i}$, $i = 1, \ldots, n$ have a multivariate Gaussian distribution.

Let X_s, $s \in \mathbb{R}$ be a stochastic process with finite second moments and assume that the covariance function $C(s, t) = \mathrm{Cov}(X_s, X_t)$ is twice continuously differentiable; then, the covariance model of the process and its mean-square derivative is given by

$$\mathrm{Cov}\left[\begin{pmatrix} X_s \\ d_s X_s \end{pmatrix}, \begin{pmatrix} X_t \\ d_t X_t \end{pmatrix}\right] = \begin{bmatrix} \mathrm{Cov}(X_s, X_t) & d_t \mathrm{Cov}(X_s, X_t) \\ d_s \mathrm{Cov}(X_s, X_t) & d_s d_t \mathrm{Cov}(X_s, X_t) \end{bmatrix}, \quad (1)$$

where $s, t \in \mathbb{R}$ (Ritter 2000). Using the linearity in the arguments the validity of this equation can be roughly seen by

$$\begin{aligned} \mathrm{Cov}(X_s, d_t X_t) &= \lim_{\Delta \to 0} \mathrm{Cov}\left(X_s, \frac{X_t - X_{t+\Delta}}{\Delta}\right) \\ &= \lim_{\Delta \to 0} \frac{\mathrm{Cov}(X_s, X_t) - \mathrm{Cov}(X_s, X_{t+\Delta})}{\Delta} \\ &= d_t \mathrm{Cov}(X_s, X_t). \end{aligned}$$

One key advantage of this approach is that the bivariate covariance in (1) allows us to model the dependence between the process and its derivative.

To provide a better theoretical basis for this idea, we consider the following definition. A stochastic process X_t, $t \in \mathbb{R}^d$ is mean-square differentiable at $t \in \mathbb{R}^d$ in direction $\mathbf{e}_i$, $i = 1, \ldots, d$, if there exists a random variable $X_t^{(i)}$ with $\mathbb{E}(X_t^{(i)})^2 < \infty$ such that

$$\mathbb{E}\left[\left(\frac{X_t - X_{t+\Delta \mathbf{e}_i}}{\Delta}\right) - X_t^{(i)}\right]^2 \to 0 \quad \text{as} \quad \Delta \to 0,$$

where $\mathbf{e}_i$ denotes the unit vector in the ith coordinate direction. In this case, we use the following notation: $(\partial/\partial \mathbf{e}_i) X_t = X_t^{(i)}$.

A stochastic process is mean-square differentiable if its covariance function is twice continuously differentiable (Ritter 2000). However, this condition is neither sufficient nor necessary for the differentiability of the sample paths. For Gaussian processes, the following conditions on the derivatives of the process guarantee continuity of the sample paths. The paths of a Gaussian process are continuous, if there exist $0 < C < \infty$ and α, $\eta > 0$ such that

$$\mathbb{E}\left|\frac{\partial}{\partial s} X_s - \frac{\partial}{\partial t} X_t\right|^2 \le \frac{C}{|\log|s - t||^{1+\alpha}},$$

for all $|s - t| < \eta$; see theorem 1.4.1. in Adler and Taylor (2007).

In our case, the covariance function describes the dependence of the horizontal wind components u_s and v_s, streamfunction ψ, velocity potential χ, and the Laplacian of the potentials (i.e., vorticity $\zeta = \Delta\psi$ and divergence $D = \Delta\chi$) at locations $\mathbf{s}, \mathbf{t} \in \mathbb{R}^2$,

$$C(\mathbf{s}, \mathbf{t}) = \mathrm{Cov}\left[\left(\psi_{\mathbf{s}}, \chi_{\mathbf{s}}, u_{\mathbf{s}}, v_{\mathbf{s}}, \Delta\psi_{\mathbf{s}}, \Delta\chi_{\mathbf{s}}\right)^{\mathrm{T}}, \left(\psi_{\mathbf{t}}, \chi_{\mathbf{t}}, u_{\mathbf{t}}, v_{\mathbf{t}}, \Delta\psi_{\mathbf{t}}, \Delta\chi_{\mathbf{t}}\right)^{\mathrm{T}}\right]. \quad (2)$$

The covariance function $C(\mathbf{s}, \mathbf{t})$ is well defined, if

$$C_{\psi,\chi}(\mathbf{s}, \mathbf{t}) = \mathrm{Cov}\left[\left(\psi_{\mathbf{s}} \chi_{\mathbf{s}}\right)^{\mathrm{T}}, \left(\psi_{\mathbf{t}} \chi_{\mathbf{t}}\right)^{\mathrm{T}}\right]$$

is four times continuously differentiable. Four times differentiability of the covariance function is equivalent to the process being twice mean-square differentiable; see lemma 14 in Ritter (2000).

In the remainder of the paper we will consider stationary processes, which means that $C(\mathbf{s}, \mathbf{t})$ depends only on the lag vector $\mathbf{h} = \mathbf{t} - \mathbf{s}$. We will adopt a commonly used notation for stationary processes: $C(\mathbf{h}) := C(0, \mathbf{h})$. Our next step is to review two notions of isotropy that exist for multivariate processes. Following Schlather et al. (2015), a vector of scalar quantities is called isotropic if the covariance function C fulfills

$$C(\mathbf{Q}\mathbf{h}) = C(\mathbf{h}) \quad \mathbf{h} \in \mathbb{R}^d, \quad (3)$$

for all rotation matrices $\mathbf{Q}$ and $\mathbf{h} = \mathbf{t} - \mathbf{s}$. A matrix $\mathbf{Q}$ is a rotation matrix if $\mathbf{Q}\mathbf{Q}^{\mathrm{T}}$ equals the d-dimensional identity matrix and $\det(\mathbf{Q}) = 1$. Under the assumption of stationarity (3) is equivalent to the more typically used notion of isotropy $C(\mathbf{h}) = C(\|\mathbf{h}\|)$. Bi- (multi) variate variables consisting of scalar quantities such as the

streamfunction, velocity potential, or the Laplacian thereof fulfill (3). A multivariate process is vector isotropic if its covariance functions fulfills

$$C(\mathbf{h}) = \mathbf{Q}^{\mathrm{T}} C(\mathbf{Q}\mathbf{h})\mathbf{Q} \quad \text{for all } \mathbf{h} \in \mathbb{R}^d. \tag{4}$$

This relation shows that $\mathbb{E}(X_0 X_{\mathbf{h}}^{\mathrm{T}}) = \mathbb{E}\left[\mathbf{Q}^{\mathrm{T}} X_0 (\mathbf{Q}^{\mathrm{T}} X_{\mathbf{Q}\mathbf{h}})^{\mathrm{T}}\right]$, which means that the covariance is preserved if the lag vector $\mathbf{h}$ and the random vector are rotated simultaneously.

In the remainder of the paper we consider isotropic processes; hence, $C_{\psi,\chi}(\mathbf{Q}\mathbf{h}) = C_{\psi,\chi}(\mathbf{h})$ for all rotation matrices $\mathbf{Q}$. Using the notation

$$\mathbf{A} = \begin{pmatrix} r_1 \cos\theta & r_1 \sin\theta \\ -r_2 \sin\theta & r_2 \cos\theta \end{pmatrix}, \tag{5}$$

we set $C_{\psi,\chi,\mathbf{A}}(\mathbf{h}) = C_{\psi,\chi}(\mathbf{A}\mathbf{h})$.

The effect of the anisotropy matrix $\mathbf{A}$ on the covariance function of the vector components—namely the rotational part $\nabla \times \psi$ and the divergent part $\nabla\chi$—is nontrivial. The divergent part satisfies

$$\mathrm{Cov}[\nabla\chi(\mathbf{A}\mathbf{s}), \nabla\chi(\mathbf{A}\mathbf{t})] = \mathbf{A}^{\mathrm{T}} \mathrm{Cov}[(\nabla\chi)(\mathbf{A}\mathbf{s}), (\nabla\chi)(\mathbf{A}\mathbf{t})]\mathbf{A}. \tag{6}$$

The rotational part fulfills a more complex formula

$$\begin{aligned} &\mathrm{Cov}[\nabla \times \psi(\mathbf{A}\mathbf{s}), \nabla \times \psi(\mathbf{A}\mathbf{t})] \\ &\quad = \mathbf{R}\mathbf{A}^{\mathrm{T}}\mathbf{R}^{\mathrm{T}} \mathrm{Cov}[(\nabla \times \psi)(\mathbf{A}\mathbf{s}), (\nabla \times \psi)(\mathbf{A}\mathbf{t})]\mathbf{R}\mathbf{A}\mathbf{R}^{\mathrm{T}}, \end{aligned} \tag{7}$$

where

$$\mathbf{R} = \begin{pmatrix} 0 & -1 \\ 1 & 0 \end{pmatrix}.$$

If $\mathbf{A}$ is simply a rotation matrix (i.e., $r_1 = r_2 = 1$), then $\mathbf{R}\mathbf{A}\mathbf{R}^{\mathrm{T}} = \mathbf{A}$, which implies that both the divergent and the rotational part are vector isotropic. For the Laplacians we obtain the following transformation

$$\begin{aligned} &\mathrm{Cov}[\Delta\chi(\mathbf{A}\mathbf{s}), \Delta\chi(\mathbf{A}\mathbf{t})] \\ &\quad = r_1^4 \mathrm{Cov}(|\partial_{e_1}^2 \chi|_{\mathbf{A}\mathbf{s}}, |\partial_{e_1}^2 \chi|_{\mathbf{A}\mathbf{t}}) + r_2^4 \mathrm{Cov}(|\partial_{e_2}^2 \chi|_{\mathbf{A}\mathbf{s}}, |\partial_{e_2}^2 \chi|_{\mathbf{A}\mathbf{t}}) \\ &\qquad + 2 r_1^2 r_2^2 \mathrm{Cov}(|\partial_{e_1}^2 \chi|_{\mathbf{A}\mathbf{s}}, |\partial_{e_2}^2 \chi|_{\mathbf{A}\mathbf{t}}). \end{aligned} \tag{8}$$

In appendix C we provide the formulas for all entries of the covariance matrix [(2)] in the isotropic case. Equations (6)–(8) are useful since they are the easiest way to compute the covariance in the anisotropic case from the covariance in the isotropic case. They have been derived using the chain rule and the linearity of the covariance function in both arguments.

Our GRF is a counterexample to a theorem of Obukhov (1954), which claims that the rotational and divergent component of isotropic vector fields are necessarily uncorrelated, which is equivalent to the streamfunction and velocity potential being uncorrelated. Obukhov considers an invalid expression for the covariance of a rotational field and deduces from this expression that it is necessarily uncorrelated to a gradient field. We present the detailed argument in appendix B.

In the remainder of the paper we will exemplify the full process in the case that the potential functions have the following bivariate structure

$$C_{\psi,\chi}(\mathbf{s}, \mathbf{t}) = \begin{pmatrix} \sigma_\psi^2 & \rho\sigma_\psi\sigma_\chi \\ \rho\sigma_\psi\sigma_\chi & \sigma_\chi^2 \end{pmatrix} M[\|\mathbf{A}(\mathbf{t} - \mathbf{s})\|_2, \nu], \tag{9}$$

where $M(\cdot, \nu)$ denotes the Matérn correlation function with smoothness parameter ν and $\|\mathbf{t} - \mathbf{s}\|_2$ the L^2 norm. Goulard and Voltz (1992) consider a more general model and prove its positive definiteness, implying the positive definiteness of our model [(9)].

Figure 1 represents a realization of the full stochastic process, with parameters chosen in order to illustrate the flexibility of the model. The rotational wind component is larger than the divergent wind component with a ratio of $\sigma_\chi/\sigma_\psi = 0.3$. The two potential functions are strongly correlated with a correlation coefficient of $\rho = 0.7$. The coherence of the variables can be very well spotted, although the simulation of the process is inherently stochastic. The smoothness is set to $\nu = 5$, which implies that not only the potentials but also vorticity and divergence are continuously differentiable. We will see later in section 4 that realistic mesoscale wind fields have a smoothness parameter close to 1.25. This suggests that the vorticity and divergence fields are discontinuous.

3. Data

The horizontal wind fields are taken from the numerical weather prediction (NWP) model COSMO-DE—namely, the wind fields at model level 20 (i.e., at approximately 7-km height). COSMO-DE is the operational version of the nonhydrostatic limited-area NWP model Consortium for Small-Scale Modeling (COSMO) operated by DWD (Baldauf et al. 2011). It provides forecasts over Germany and surrounding countries on a 2.8-km horizontal grid and 50 vertical levels. At this grid size, deep convection is permitted by the dynamics, and COSMO-DE is able to generate deep convection without an explicit parameterization thereof. Thus, COSMO-DE particularly aims at the prediction of mesoscale convective precipitation with a forecast

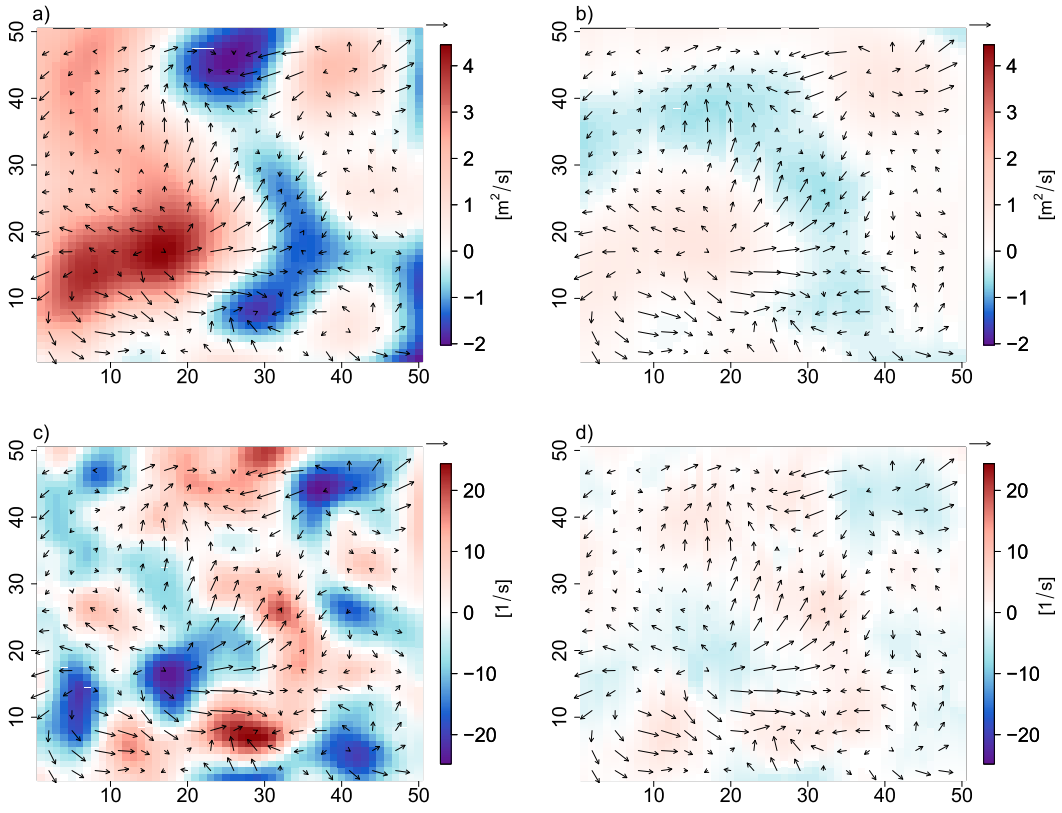

FIG. 1. Isotropic realization of the multivariate GRF with parameters $\nu = 5$, $\sigma_\chi/\sigma_\psi = 0.3$, $\rho = 0.7$, and $r_1 = r_2 = 0.25$. Color shadings are the (a) streamfunction, (b) velocity potential, (c) vorticity, and (d) divergence. The arrows represent the associated wind fields ($\mathrm{m\,s^{-1}}$). The arrow in the upper-right corner is a standard arrow of $0.5\,\mathrm{m\,s^{-1}}$. The x and y axes indicate distance measured in grid points.

horizon of up to 1 day. The ensemble prediction system (COSMO-DE-EPS) uses COSMO-DE with different lateral boundary conditions (LBC), perturbed initial conditions, and slightly modified parameterizations. The four LBCs are generated by the Global Forecast Systems of NCEP, the Global Model of DWD, the Integrated Forecast System of ECMWF, and the Global Spectral Model of the Meteorological Agency of Japan. For details on the setup of COSMO-DE-EPS, the reader is referred to Gebhardt et al. (2011), Peralta et al. (2012), and references therein.

In our application we concentrate on a COSMO-DE forecast for 1200 UTC 5 June 2011 initialized at 0000 UTC. COSMO-DE-EPS provides 20 forecasts of horizontal wind fields on a grid with 461 × 421 grid points. Five ensemble members are forced with identical LBCs, respectively. They only differ as a result of perturbed initial conditions and four different parameterizations. Thus differences between the members with identical LBCs are mainly due to small-scale internal dynamics. These differences are the differences obtained from subtracting two fields that have been generated using the same lateral boundary conditions. All combinations of fields with different model physics and identical lateral boundary conditions generate a set of 40 different fields of differences. The differences are referred to as inner-LBC anomalies.

To illustrate the data, Fig. 2 displays a field of inner-LBC anomalies of the zonal wind component. The fields exhibit small-scale anomalies with amplitudes that vary over the model region while the spatial structure seems relatively homogeneous. Thus, the data violate the assumption of stationarity. To model the instationarity of the variance we estimate the spatial kinetic energy $\hat{g}$ by applying a kernel smoother to the kinetic energy field. Analogous to the field of electric susceptibility $(1 + \chi_e)$, which models the spatial-varying potential polarization of the dielectric medium (Jackson 1962), we apply the following transformation to the data:

$$\tilde{U}_{\mathbf{s}} = \frac{U_{\mathbf{s}}}{c + \hat{g}_{\mathbf{s}}},$$

where $c \in \mathbb{R}_+$. Such a transformation, if applied to the full field $(\tilde{\chi}, \tilde{\psi}, \tilde{U}, \tilde{D}, \tilde{\zeta}) = (\chi, \psi, U, D, \zeta)/(c + \hat{g})$, violates the differential relations that hold between the

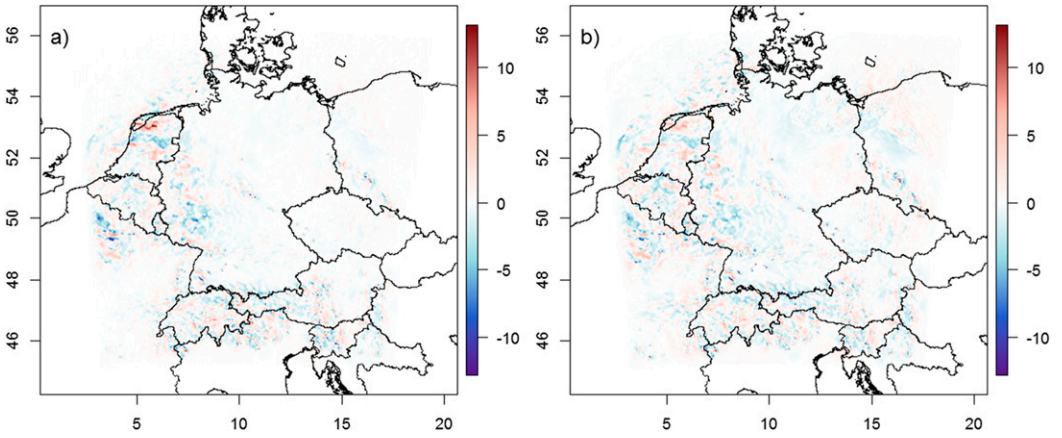

FIG. 2. Zonal wind component at 1200 UTC 5 Jun 2011. (a) The inner-LBC anomalies and (b) the transformed inner-LBC anomalies. The colors represent wind speed ($\mathrm{m\,s^{-1}}$). The x and y axes are in longitude and latitude.

variables, though they are still valid approximately. For example, for a nonrotational field, we have

$$\nabla\left(\frac{\chi}{c+\hat{g}}\right)=\frac{\nabla\chi}{c+\hat{g}}+\varepsilon. \tag{10}$$

The smoother the transformation the smaller the approximation error:

$$\varepsilon=-\frac{\chi\nabla(c+\hat{g})}{(c+\hat{g})^2}.$$

Because of the constant $c>0$, the transformation [(10)] does not resolve the full instationarity of the data. Still we find that this transformation is superior to the more natural transformation $\tilde{U}=U/\hat{g}$, as the approximation error for the potential functions is strongly reduced by the introduction of $c>0$. We observe a trade-off between the differential relations being hardly violated and on the other side Gaussian marginal distribution and constant variance in space by a rougher function $\hat{g}$ and values of c close to zero. We chose $c=1/3$ and a kernel such that the transformation kurtosis of the data is reduced from 24 to 16, while we have to accept an error of the potential fields close to 15%. The error is measured by comparing the potential that satisfies $\nabla\tilde{\chi}=U/(c+\hat{g})$ and the potential that satisfies $\nabla\chi=U$ and is normalized by $c+\hat{g}$ (the same is done for the rotational part). Figure 2 shows that the instationarity of the original fields is mitigated by the transformation. Figure 3 shows the marginal distribution of the transformed inner-LBC anomalies for the zonal and the meridional wind components. Both distributions deviate from the assumption of Gaussian marginals, although Gaussianity is a common assumption for wind fields in the meteorological literature (Frehlich et al. 2001). The kurtosis amounts to about 16 instead of 3, which results in heavier extreme values than expected under the assumption of Gaussianity.

4. Parameter estimation

We start by parameter estimation of the bivariate GRF model for the transformed inner-LBC anomalies of the horizontal wind fields described in section 3. Since the computation of the Gaussian likelihood would require the inversion of a quadratic matrix with $2\times461\times421$ rows, a standard maximum likelihood approach is unfeasible. We thus use a composite likelihood (CL) approach to approximate the true likelihood function. An overview of the CL approach is given in Varin et al. (2011). Here, we apply a special version of the CL approach known as pairwise likelihood (Cox and Reid 2004). For a bivariate field, this likelihood is a product of four-dimensional likelihoods. We calculate the log likelihood of the CL as

$$l^c(\boldsymbol{\theta})=\sum_{\mathbf{s}\in\mathbb{G}}\sum_{\mathbf{h}\in N}\log[L(u_{\mathbf{s}},v_{\mathbf{s}},u_{\mathbf{s}+\mathbf{h}},v_{\mathbf{s}+\mathbf{h}}|\boldsymbol{\theta})],$$

where $\boldsymbol{\theta}$ denotes the parameter vector and $\mathbb{G}$ denotes the set of all grid points. The set N controls for which separations $\mathbf{h}$ the likelihood is computed. The set N has to be determined relative to the given problem. If feasible, it should include all lags $\mathbf{h}$ for which there is nonnegligible dependence and some for which there is negligible dependence, in order to estimate the range. One way of determining this is to inspect the empirical covariance estimate. We chose N to be a regular 41×41 grid with step size one, which is centered in the origin. The choice is justified by the low uncertainties observed in the parametric bootstrap samples presented below.

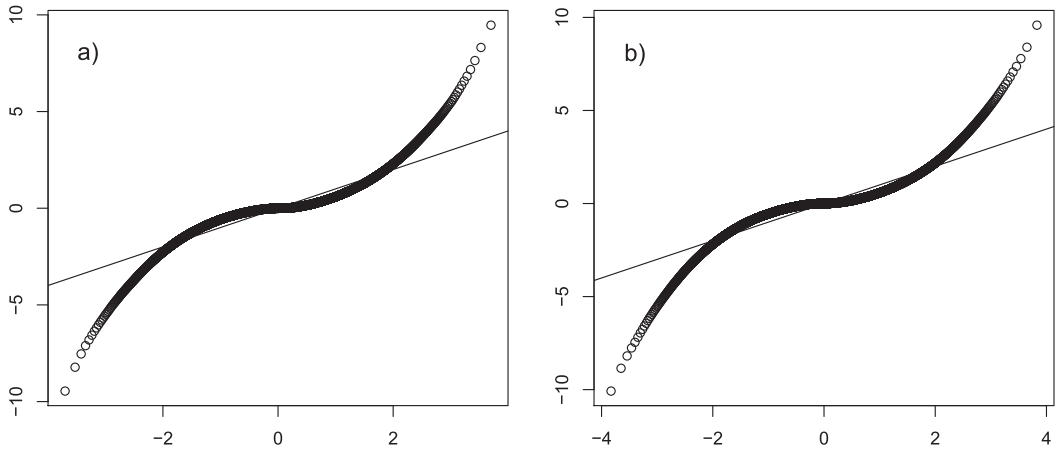

FIG. 3. Quantile–quantile plot of the (a) zonal and (b) meridional wind component of transformed inner-LBC anomalies vs a standard normal distribution. The straight lines indicate perfect accordance with the marginal distributions; both graphs depict clear deviation from the normal distribution.

The unknown parameters are the variances of the potentials σ_ψ^2 and σ_χ^2, their correlation ρ, the smoothness parameter ν, and the scale parameters r_1, r_2, and the angle θ of the anisotropy.

To reduce the number of parameters, we use the correlation function instead of the covariance function, which only depends on the ratio and not on the magnitude of the variances of streamfunction and velocity potential (Daley 1991). This is possible as we can estimate the variance of the zonal and meridional wind with very low uncertainty owing to the large size of the considered grid.

CL was maximized using the built-in function "optim" of R Core Team (2015). To show the independence of the optimization technique of the initial values it was started 50 times with varying initial parameters. This reveals that there is a single global maximum of the likelihood function.

Parameter uncertainty such as the Fisher information is not available for our problem. We thus resort to a parametric bootstrap (Efron and Tibshirani 1994) to assess uncertainty of the parameter estimates. We simulated the multivariate GRF using circulant embedding (Wood and Chan 1994) to obtain independent realizations of the fitted process. Reestimating the parameters for a sample of 100 independent realizations provides the uncertainty of the parameter estimates given that the estimated model is true. The simulation of the data was made possible by the implementation of the considered covariance model in an upcoming version of the spatial statistics package RandomFields (Schlather et al. 2016). The parametric bootstrap describes the estimation uncertainty based on the assumption that the model is sufficiently close to the data. It cannot assess the uncertainty related to the modeling error. As the considered data deviates from a Gaussian distribution and is only approximately stationary, this error is presumably not negligible.

5. Results

Figure 4 shows the estimates of the parameters of the multivariate GRF and the respective distribution of the parametric bootstrap estimates as a boxplot. The ratio of divergent and rotational wind is estimated to about $\sigma_\chi/\sigma_\psi \approx 0.82$. This indicates that both wind components are of the same order of magnitude. A geostrophic balance would require a ratio of order $\sigma_\chi/\sigma_\psi = 0.1$, with a significant dominance of the rotational wind component. This is not the case in COSMO-DE, which is well consistent with the mesoscale dynamics, which are highly nongeostrophic. The results are also consistent with L. B. Bierdel (2012, personal communication). Her spectral analysis of the horizontal wind fields of COSMO-DE-EPS revealed a slightly stronger rotational than divergent component.

Figure 4b compares the statistical estimate for $\lambda = \sigma_\chi/\sigma_\psi$ to a numeric estimate, which equals the ratio of the L^2 norms of curl and divergence of the wind field calculated with finite difference approximations and that is denoted by λ_N. Both estimators have been computed on data simulated by our model [(9)]. The comparison made for the two estimators has the limitation of the parametric bootstrap described in section 4. The uncertainty related to the modeling error cannot be quantified by it. Yet the performance on data simulated by our model can be assessed. Although the statistical estimate has a higher variance, it clearly outperforms the numeric estimate owing to the relatively large bias of the latter on data simulated from our model. Our model can be used to

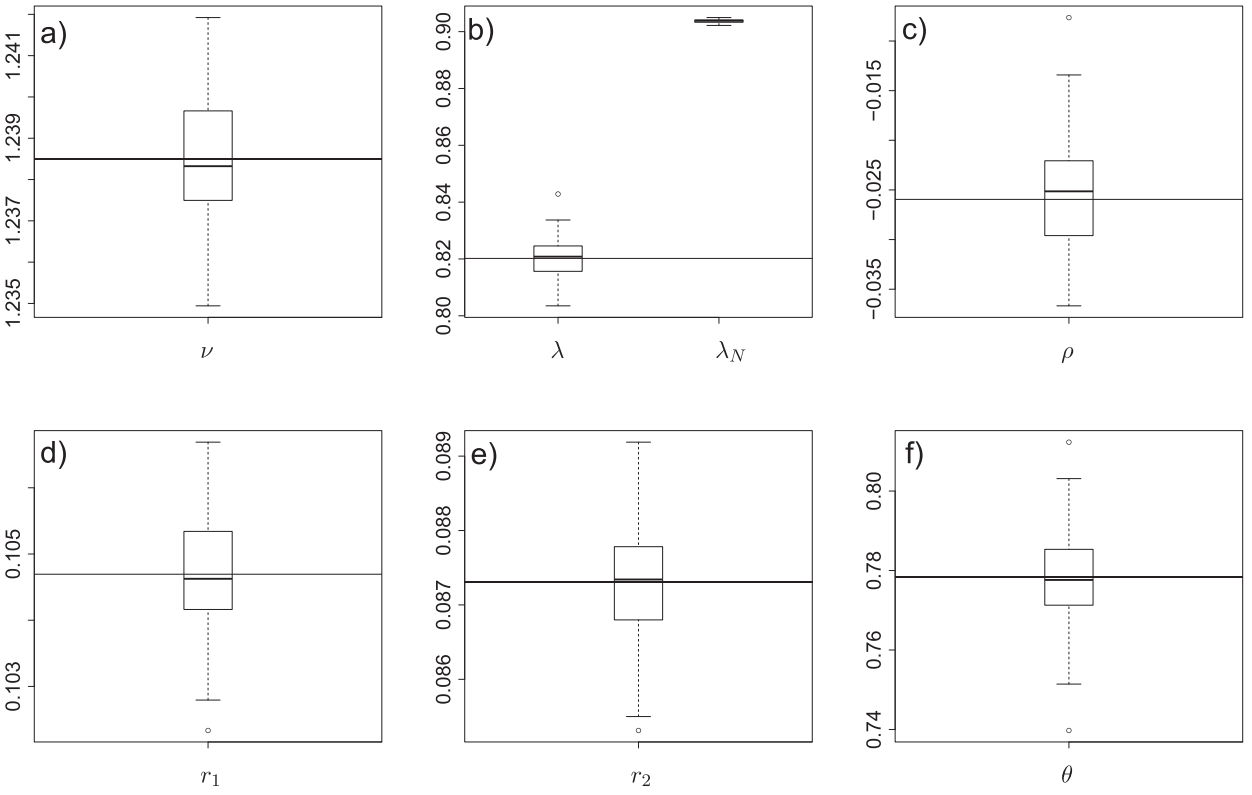

FIG. 4. Box-and-whisker plots representing the parametric bootstrap estimates for the inner-LBC wind anomalies. The horizontal lines indicate the maximum likelihood (ML) estimate values: (a) the smoothness parameter ν and (b) the left plot shows ML estimates λ and the right plot shows the numerically derived estimates λ_N of the ratio $\lambda = \sigma_\chi/\sigma_\psi$. (c) The correlation ρ, (d) the scale parameter r_1, (e) the scale parameter r_2, and (f) the angle of the anisotropy matrix θ.

generate data with known parameters and based on this data the performance of estimators can be assessed.

The correlation between the streamfunction and velocity potential ρ is almost zero ($\approx -2.5 \times 10^{-2}$). Similar results have been described for larger scales (Hollingsworth and Lönnberg 1986) and have often been assumed in the literature (Daley 1991). The smoothness parameter ν is close to 1.24. This corresponds to noncontinuous fields of vorticity and divergence. This relatively low value of ν is not due to noise in the data. We have included tentatively a noise parameter in the estimation but it was set to zero (not shown). As a measure for the anisotropy we consider the ratio of the scale parameters r_1/r_2. This ratio is significant larger than 1 for both datasets, which suggests that the data are anisotropic. The estimated parameters are very much in accordance with our expectations, as they describe a nongeostrophic and anisotropic wind field. The most important result is that the independence of the streamfunction and velocity potential in the case of the 5 June 2011 is valid on the mesoscale. Similar results were already known for larger scales (Hollingsworth and Lönnberg 1986). In addition, our parametric bootstrap reveals that this covariance model can be estimated with a very high precision if the distribution of the data is close to the model. Under the same condition we have shown that our estimate of the ratio of divergence and vorticity is superior to a numeric estimate.

Figure 5 shows the empirical estimate of the correlation structure of the data and the correlation obtained for the maximum likelihood estimation. Again the scale and the orientation of the correlation are very well matched. The (u, u) and (v, v) autocorrelation component is matched relatively well. The (u, v) correlation component has a deviation from the data as there are regions of positive correlation, which is not present in the empirical correlation estimate.

The implementation of our covariance model in an upcoming version of the R package RandomFields (Schlather et al. 2016) allows for the simulation of large field with a size of the order of 800×800 grid points. This is made feasible by using circulant embedding introduced by Wood and Chan (1994). Circulant embedding is a powerful simulation technique, which to the best of our knowledge, has not been used for the simulation of wind fields yet.

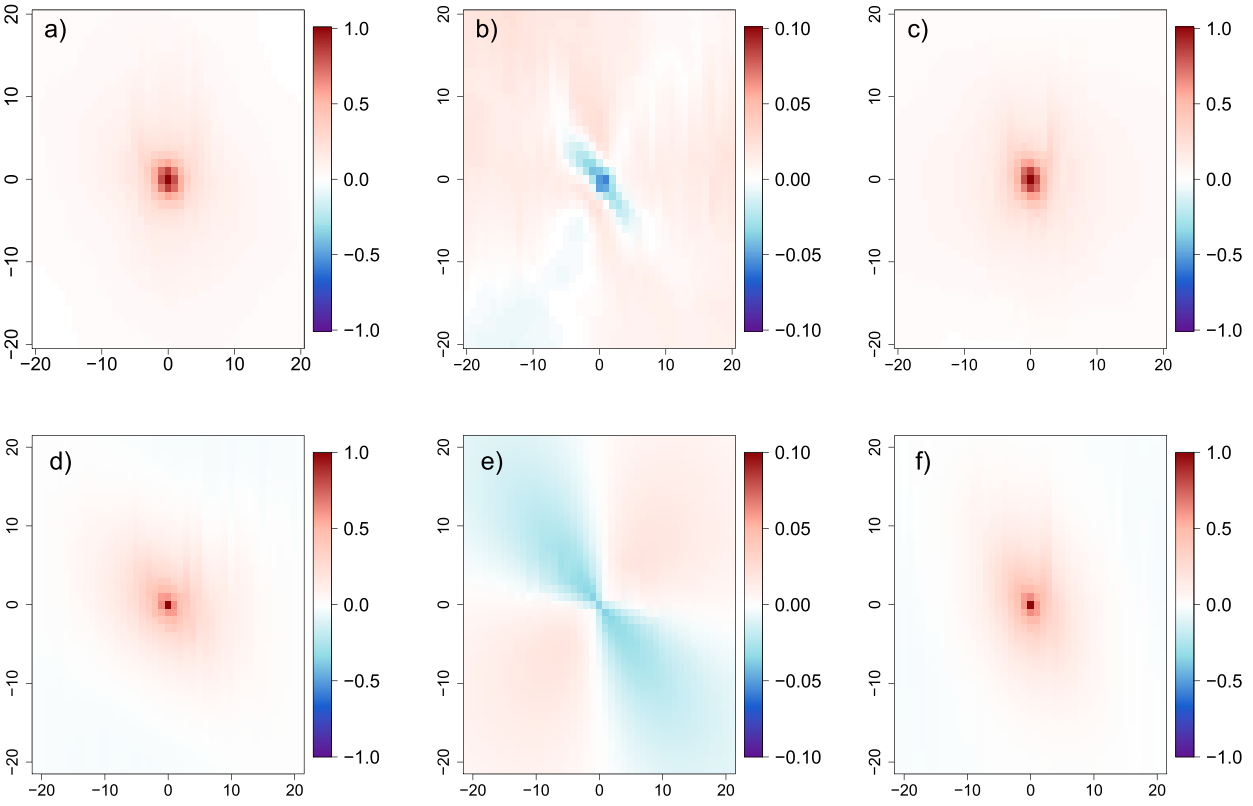

FIG. 5. (top) Empirical correlation for (a) (u, u), (b) (u, v), and (c) (v, v) and (bottom) estimated correlation for (d) (u, u), (e) (u, v), and (f) (v, v) for dataset 1.

Figure 6 shows the zonal wind anomalies from Fig. 2 together with a realization of the fitted multivariate GRF, which has been scaled with the spatial variance that has not been resolved by the transformation [(10)]. It shows that the orientation as well as the spatial scale of the zonal wind fields matches very well. The multivariate GRF shows less extreme values and fewer values very close to zero, owing to the assumption of Gaussianity. However, visual accordance is quite good, such that we conclude that the multivariate GRF formulation represents a useful stationary, multivariate Gaussian random fields approximation of mesoscale wind anomalies.

6. Conclusions

In this paper we introduce a multivariate GRF that jointly models the streamfunction, velocity potential, the two-dimensional wind field, vorticity, and divergence. Its flexibility allows for different variances of the potential functions, anisotropy, and a flexible smoothness parameter. Further, the model is able to represent nonzero correlation of the divergent and nondivergent wind components. All parameters of the proposed covariance model have direct meteorological interpretation, such that they provide meteorological insight into the dynamics of the atmosphere. Further, the model allows us to easily implement meteorological balances such as nondivergence or geostrophy.

We have reviewed the theory that guarantees the existence of derivatives of stochastic processes, developed a complex covariance model for various atmospheric variables, and studied its transformation subject to anisotropy. Our multivariate GRF is a counterexample to a theorem of Obukhov (1954), which claims that the rotational and divergent components of an isotropic vector field are necessarily uncorrelated.

We have developed an estimation technique and shown its performance for wind anomalies of a mesoscale ensemble prediction system (COSMO-DE-EPS). A parametric bootstrap method provides estimates of the uncertainty implicit in our estimation technique. We thus provide estimates for the ratio of variances of the rotational and divergent wind components without numerical approximations. Numeric estimates suffer from a truncation error, which arises owing to the numerical scheme that computes the derivatives of the wind field.

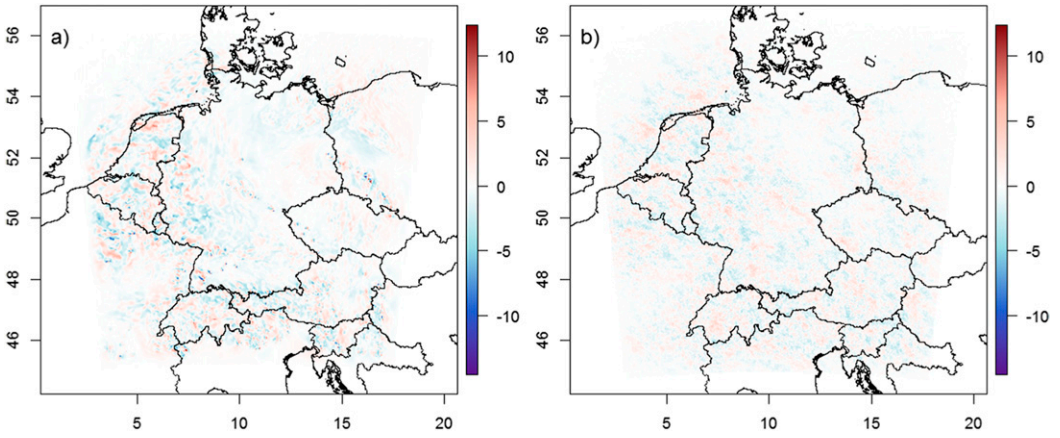

FIG. 6. (a) As in Fig. 2b. (b) Zonal wind component of a realization of the fitted GRF. The x and y axes are in longitude and latitude.

The multivariate GRF formulation may be particularly useful for global atmospheric models with a spectral representation of the horizontal fields, such as the ECHAM climate model (Roeckner et al. 2003). Spectral models solve the prognostic equations for the potentials instead of the horizontal wind components, whereas the observations are given as horizontal wind vectors. Our multivariate GRF formulation provides a consistent formulation of the covariance structure for both the potential and the horizontal wind components. A stochastic formulation of the potentials may also be relevant for the assimilation of measurements of the vertical velocity (Bühl et al. 2015), which provide proxies for the horizontal divergence of the field. Our covariance function represents the divergence within a stochastic model, which is needed to assimilate the observations.

The proposed covariance model can be used to interpolate observed wind fields and to compute the associated derivative fields. This is feasible either by conditional simulation or kriging. Numerical methods have been used for interpolation (Schaefer and Doswell 1979) and the computation of derivatives of vector fields (Caracena 1987; Doswell and Caracena 1988). While numeric methods become significantly more complex for scattered observations, the multivariate GRF formulation provides an accessible way for both problems, which additionally provides information about the uncertainty.

The fields obtained by computing the expectation of vector potential and the streamfunction given a certain wind field can be shown to solve the differential equations of the Helmholtz equation. In this sense, our covariance model can be used via kriging to solve the Helmholtz equation. As stochastic models describe the uncertainty of all of the variables, these methods even allow stochastic error bands to be computed for the solution of the partial differential equations.

Another potential application is the stochastic simulation of the transport of tracer variables such as aerosols or humidity in the atmosphere. Stochastic models that describe gradient fields and their divergence have been considered in the literature (Scheuerer and Schlather 2012). However, to the best of our knowledge no stochastic model has been formulated to jointly model spatial wind fields and its divergence. Both variables are needed to describe the transport adequately.

Our methods show that both physical coherence and geostrophic constraints can be easily implemented into a covariance model. Further, we have illustrated that the model parameters can be estimated with very small uncertainty on data simulated by our model.

Acknowledgments. Rüdiger Hewer was funded by VolkswagenStiftung within the project ''Mesoscale Weather Extremes: Theory, Spatial Modeling and Prediction (WEX-MOP).'' Data used in this study are kindly provided by the German Meteorological Service (DWD). We thank Chris Snyder and an anonymous reviewer for the thoughtful comments, which improved our paper substantially. We are especially grateful to the reviewer for the idea to transform the data such that our model assumptions are more appropriate. We thank Sebastian Buschow for help in preparing the data.

APPENDIX A

Positive Definiteness of Daley's Model

Daley (1985) proposed the covariance model (cf. Moreva and Schlather 2016; Gneiting et al. 2010)

$$\mathbf{C}(r) = \begin{Bmatrix} \exp\left(-\frac{1}{2}r^2\right) & \lambda \exp\left[-\frac{1}{2}\left(\frac{r}{a}\right)^2\right] \\ \lambda \exp\left[-\frac{1}{2}\left(\frac{r}{a}\right)^2\right] & \exp\left[-\frac{1}{2}\left(\frac{r}{a}\right)^2\right] \end{Bmatrix}, \quad r = \|\mathbf{h}\|,$$

for the streamfunction and velocity potential. The Fourier transform of this covariance matrix is given by

$$\widehat{\mathfrak{F}}(\mathbf{C})(\varphi) = \begin{Bmatrix} \exp\left(-\frac{1}{2}\varphi^2\right) & \frac{\lambda}{a}\exp\left[-\frac{1}{2}\left(\frac{\varphi}{a}\right)^2\right] \\ \frac{\lambda}{a}\exp\left[-\frac{1}{2}\left(\frac{\varphi}{a}\right)^2\right] & \frac{1}{a}\exp\left[-\frac{1}{2}\left(\frac{\varphi}{a}\right)^2\right] \end{Bmatrix}.$$

By Cramér's theorem (Chiles and Delfiner 2009) this Fourier transform needs to be positive definite for almost all frequencies φ. This is equivalent to

$$\det[\widehat{\mathfrak{F}}(\mathbf{C})(\varphi)] \geq 0 \quad \forall \varphi \in \mathbb{R},$$

a condition equivalent to

$$\exp\left[-\frac{1}{2}\varphi^2\left(1-\frac{1}{a^2}\right)\right] \geq \frac{\lambda^2}{a} \quad \forall \varphi \in \mathbb{R}.$$

If $a > 1$, the model is not positive definite unless $\lambda = 0$. If $0 < a \leq 1$, the model is positive definite if $a \geq \lambda^2$. Daley proposed $a > 1$ such that the model does not allow a nonzero correlation.

APPENDIX B

Obukhov's Independence Claims

Obukhov (1954) presents two arguments for an isotropic rotational field having zero correlation with an isotropic scalar field and with an isotropic gradient field. We believe that both arguments are erroneous for the same reason. As the argument for the scalar field is much less involved, we restrict ourselves to this case. Obukhov claims that the covariance of an isotropic rotational field to an arbitrary scalar isotropic variable is of the form $\mathrm{Cov}(\chi_{\mathbf{s}}, \nabla \times \psi_{\mathbf{s}+\mathbf{h}}) = P(\|\mathbf{h}\|)\mathbf{h}/\mathbf{h}$ for some function P. Using the nondivergence of a rotational field, Obukhov deduces from his assumption the following:

$$0 = \mathbb{E}(\chi_{\mathbf{s}} \nabla \cdot \nabla \times \psi_{\mathbf{s}+\mathbf{h}}) = \nabla \cdot \mathbb{E}(\chi_{\mathbf{s}} \nabla \times \psi_{\mathbf{s}+\mathbf{h}})$$
$$= \nabla \cdot \left[\frac{P(\|\mathbf{h}\|)}{\mathbf{h}}\begin{pmatrix} h_1 \\ h_2 \end{pmatrix}\right] = \frac{2P(\mathbf{h})}{\mathbf{h}} + \frac{\partial}{\partial\|\mathbf{h}\|}\left[\frac{P(\mathbf{h})}{\|\mathbf{h}\|}\right]\|\mathbf{h}\|$$
$$= \frac{P(\|\mathbf{h}\|)}{\mathbf{h}} + P'(\|\mathbf{h}\|).$$

This differential equation is solved by the function

$$P(\|\mathbf{h}\|) = \frac{c}{\mathbf{h}} \quad c \in \mathbb{R}.$$

If $c \neq 0$, this function has a pole. This implies that the variance of the corresponding field could not exist. Hence, $c = 0$ and this again implies the zero correlation between the scalar field and the rotational field.

We believe that the correct covariance of a scalar field and a rotational field is given by

$$\mathrm{Cov}(\chi_{\mathbf{s}}, \nabla \times \psi_{\mathbf{s}+\mathbf{h}}) = \frac{P(\|\mathbf{h}\|)}{\mathbf{h}}\begin{pmatrix} -h_2 \\ h_1 \end{pmatrix},$$

for some P, as the curl operator derives the first component in direction $\mathbf{e}_2$ and the second in direction $\mathbf{e}_1$. This covariance is consistent with the anisotropic transformation of the field, which has been described in (7). Using this assumption the independence of an isotropic scalar field and an isotropic rotational field cannot be deduced. However,

$$\mathbb{E}(\chi_{\mathbf{s}} \nabla \cdot \nabla \times \psi_{\mathbf{s}+\mathbf{h}}) = \nabla \cdot \mathbb{E}(\chi_{\mathbf{s}} \nabla \times \psi_{\mathbf{s}+\mathbf{h}})$$
$$= \nabla \cdot \left[\frac{P(\|\mathbf{h}\|)}{\|\mathbf{h}\|}\begin{pmatrix} -h_2 \\ h_1 \end{pmatrix}\right]$$
$$= \frac{P(\|\mathbf{h}\|)}{\|\mathbf{h}\|^2}(-h_2 h_1 + h_1 h_2) = 0$$

for any differentiable function P.

APPENDIX C

Formulas of the Isotropic Covariance Model

We describe the formula for the covariance function considered in this paper [(2)]. For brevity, we introduce the following notation:

$$X_{1,\mathbf{s}} := \psi_{\mathbf{s}} X_{2,\mathbf{s}} := \chi_{\mathbf{s}},$$
$$U_{1,\mathbf{s}} := u_{\mathbf{s}} U_{2,\mathbf{s}} := v_{\mathbf{s}}, \quad \text{and}$$
$$\partial_i := \partial_{\mathbf{e}_i},$$

and omit the argument of the covariance functions, which is $(\mathbf{t} - \mathbf{s})$ in all of the following cases:

$$C^{i,j} := \mathrm{Cov}(X_{i,\mathbf{s}}, X_{j,\mathbf{t}}),$$

$$\mathrm{Cov}(U_{i,\mathbf{s}}, U_{j,\mathbf{t}}) = (-1)^{i+j}\frac{\partial^2}{\partial_{3-i}\partial_{3-j}}C^{1,1} + (-1)^i\frac{\partial}{\partial_{3-i}\partial_j}C^{1,2}$$
$$+ (-1)^j\frac{\partial^2}{\partial_i\partial_{3-j}}C^{2,1} + \frac{\partial}{\partial_i\partial_j}C^{2,2},$$

$$\mathrm{Cov}(\Delta X_{i,\mathbf{s}}, \Delta X_{j,\mathbf{t}}) = \sum_{(k,l)\in\{1,2\}^2} \frac{\partial^4}{\partial_k^2 \partial_l^2} C^{i,j},$$

$$\mathrm{Cov}(U_{i,\mathbf{s}}, X_{j,\mathbf{t}}) = -\mathrm{Cov}(X_{j,\mathbf{s}}, U_{i,\mathbf{t}}) = (-1)^i \frac{\partial}{\partial e_{3-i}} C^{1,j} + \frac{\partial}{\partial e_i} C^{2,j},$$

$$\mathrm{Cov}(X_{i,\mathbf{s}}, \Delta X_{j,\mathbf{t}}) = \mathrm{Cov}(\Delta X_{j,\mathbf{s}}, X_{i,\mathbf{t}}) = \frac{\partial^2}{\partial^2 e_1} C^{i,j} + \frac{\partial^2}{\partial^2 e_2} C^{i,j}, \quad \text{and}$$

$$\mathrm{Cov}(U_{i,\mathbf{s}}, \Delta X_{j,\mathbf{t}}) = -\mathrm{Cov}(\Delta X_{j,\mathbf{s}}, U_{i,\mathbf{t}}) = (-1)^i \frac{\partial^3}{\partial_{3-i} \partial_1^2} C^{1,j} + (-1)^i \frac{\partial^3}{\partial_{3-i} \partial_2^2} C^{1,j} + \frac{\partial^3}{\partial_i \partial_1^2} C^{2,j} + \frac{\partial^3}{\partial_i \partial_2^2} C^{2,j},$$

where $i, j \in \{1, 2\}$.

REFERENCES

Adler, R. J., and J. E. Taylor, 2007: *Random Fields and Geometry*. Springer Monographs in Mathematics, Vol. 17, Springer, 448 pp., doi:10.1007/978-0-387-48116-6.

Baldauf, M., A. Seifert, J. Förstner, D. Majewski, M. Raschendorfer, and T. Reinhardt, 2011: Operational convective-scale numerical weather prediction with the COSMO model: Description and sensitivities. *Mon. Wea. Rev.*, **139**, 3887–3905, doi:10.1175/MWR-D-10-05013.1.

Bannister, R. N., 2008: A review of forecast error covariance statistics in atmospheric variational data assimilation. II: Modelling the forecast error covariance statistics. *Quart. J. Roy. Meteor. Soc.*, **134**, 1971–1996, doi:10.1002/qj.340.

Bierdel, L., C. Snyder, S.-H. Park, and W. C. Skamarock, 2016: Accuracy of rotational and divergent kinetic energy spectra diagnosed from flight-track winds. *J. Atmos. Sci.*, **73**, 3273–3286, doi:10.1175/JAS-D-16-0040.1.

Bonavita, M., L. Isaksen, and E. Hólm, 2012: On the use of EDA background error variances in the ECMWF 4D-Var. *Quart. J. Roy. Meteor. Soc.*, **138**, 1540–1559, doi:10.1002/qj.1899.

Bühl, J., R. Leinweber, U. Görsdorf, M. Radenz, A. Ansmann, and V. Lehmann, 2015: Combined vertical-velocity observations with Doppler lidar, cloud radar and wind profiler. *Atmos. Meas. Tech.*, **8**, 3527–3536, doi:10.5194/amt-8-3527-2015.

Bühler, O., J. Callies, and R. Ferrari, 2014: Wave–vortex decomposition of one-dimensional ship-track data. *J. Fluid Mech.*, **756**, 1007–1026, doi:10.1017/jfm.2014.488.

Caracena, F., 1987: Analytic approximation of discrete field samples with weighted sums and the gridless computation of field derivatives. *J. Atmos. Sci.*, **44**, 3753–3768, doi:10.1175/1520-0469(1987)044<3753:AAODFS>2.0.CO;2.

Chiles, J.-P., and P. Delfiner, 2009: *Geostatistics: Modeling Spatial Uncertainty*. Wiley Series in Probability and Statistics, Vol. 497, Wiley, 699 pp.

Cox, D. R., and N. Reid, 2004: A note on pseudolikelihood constructed from marginal densities. *Biometrika*, **91**, 729–737, doi:10.1093/biomet/91.3.729.

Daley, R., 1985: The analysis of synoptic scale divergence by a statistical interpolation procedure. *Mon. Wea. Rev.*, **113**, 1066–1080, doi:10.1175/1520-0493(1985)113<1066:TAOSSD>2.0.CO;2.

——, 1991: *Atmospheric Data Analysis*. 2nd ed. Cambridge University Press, 457 pp.

Doswell, C. A., III, and F. Caracena, 1988: Derivative estimation from marginally sampled vector point functions. *J. Atmos. Sci.*, **45**, 242–253, doi:10.1175/1520-0469(1988)045<0242:DEFMSV>2.0.CO;2.

Efron, B., and R. J. Tibshirani, 1994: *An Introduction to the Bootstrap*. Chapman & Hall, 456 pp.

Evensen, G., 1994: Sequential data assimilation with a nonlinear quasi-geostrophic model using Monte Carlo methods to forecast error statistics. *J. Geophys. Res.*, **99**, 10 143–10 162, doi:10.1029/94JC00572.

Frehlich, R., L. Cornman, and R. Sharman, 2001: Simulation of three-dimensional turbulent velocity fields. *J. Appl. Meteor.*, **40**, 246–258, doi:10.1175/1520-0450(2001)040<0246:SOTDTV>2.0.CO;2.

Gandin, L. S., 1965: *Objective Analysis of Meteorological Fields*. Israel Program for Scientific Translations, 242 pp.

Gebhardt, C., S. Theis, M. Paulat, and Z. B. Bouallégue, 2011: Uncertainties in COSMO-DE precipitation forecasts introduced by model perturbations and variation of lateral boundaries. *Atmos. Res.*, **100**, 168–177, doi:10.1016/j.atmosres.2010.12.008.

Gneiting, T., W. Kleiber, and M. Schlather, 2010: Matérn cross-covariance functions for multivariate random fields. *J. Amer. Stat. Assoc.*, **105**, 1167–1177, doi:10.1198/jasa.2010.tm09420.

Goulard, M., and M. Voltz, 1992: Linear coregionalization model: Tools for estimation and choice of cross-variogram matrix. *Math. Geol.*, **24**, 269–286, doi:10.1007/BF00893750.

Hollingsworth, A., and P. Lönnberg, 1986: The statistical structure of short-range forecast errors as determined from radiosonde data. Part I: The wind field. *Tellus*, **38A**, 111–136, doi:10.1111/j.1600-0870.1986.tb00460.x.

Jackson, J. D., 1962: *Electrodynamics*. Wiley, 641 pp.

Kalnay, E., 2003: *Atmospheric Modeling, Data Assimilation and Predictability*. Cambridge University Press, 341 pp.

Kolmogorov, A. N., 1941: The local structure of turbulence in incompressible viscous fluid for very large Reynolds numbers. *Dokl. Akad. Nauk SSSR*, **31**, 538–540.

Lindborg, E., 2015: A Helmholtz decomposition of structure functions and spectra calculated from aircraft data. *J. Fluid Mech.*, **762**, R4-1–R4-11, doi:10.1017/jfm.2014.685.

Moreva, O., and M. Schlather, 2016: Modeling and simulation of bivariate Gaussian random fields. arXiv.org, 16 pp., https://arxiv.org/abs/1609.06561.

Obukhov, A., 1954: Statistical description of continuous fields. *Tr. Geofiz. Inst., Akad. Nauk. SSSR*, **24**, 3–42.

Peralta, C., Z. Ben Bouallègue, S. Theis, C. Gebhardt, and M. Buchhold, 2012: Accounting for initial condition uncertainties in COSMO-DE-EPS. *J. Geophys. Res.*, **117**, D07108, doi:10.1029/2011JD016581.

Pu, Z., S. Zhang, M. Tong, and V. Tallapragada, 2016: Influence of the self-consistent regional ensemble background error covariance on hurricane inner-core data assimilation with the GSI-based hybrid system for HWRF. *J. Atmos. Sci.*, **73**, 4911–4925, doi:10.1175/JAS-D-16-0017.1.

R Core Team, 2015: *R: A Language and Environment for Statistical Computing*. R Foundation for Statistical Computing, https://www.R-project.org/.

Ritter, K., 2000: *Average-Case Analysis of Numerical Problems*. Lecture Notes in Mathematics, Vol. 1733, Springer, 225 pp.

Roeckner, E., and Coauthors, 2003: The atmospheric general circulation model ECHAM5. Part I: Model description. Max Planck Institute for Meteorology Tech. Rep. 349, 127 pp., http://www.mpimet.mpg.de/fileadmin/models/echam/mpi_report_349.pdf.

Royle, J. A., L. M. Berliner, C. K. Wikle, and R. Milliff, 1999: A hierarchical spatial model for constructing wind fields from scatterometer data in the Labrador Sea. *Case Studies in Bayesian Statistics*, Vol. IV, C. Gatsonis et al., Eds., Springer, 367–382.

Schaefer, J. T., and C. A. Doswell III, 1979: On the interpolation of a vector field. *Mon. Wea. Rev.*, **107**, 458–476, doi:10.1175/1520-0493(1979)107<0458:OTIOAV>2.0.CO;2.

Scheuerer, M., and M. Schlather, 2012: Covariance models for divergence-free and curl-free random vector fields. *Stochastic Models*, **28**, 433–451, doi:10.1080/15326349.2012.699756.

Schlather, M., A. Malinowski, P. J. Menck, M. Oesting, and K. Strokorb, 2015: Analysis, simulation and prediction of multivariate random fields with package randomfields. *J. Stat. Software*, **63**, 1–25, doi:10.18637/jss.v063.i08.

——, and Coauthors, 2016: Randomfields: Simulation and analysis of random fields, version 3.1.16. R package, http://ms.math.uni-mannheim.de/de/publications/software.

Thiébaux, H. J., 1977: Extending estimation accuracy with anisotropic interpolation. *Mon. Wea. Rev.*, **105**, 691–699, doi:10.1175/1520-0493(1977)105<0691:EEAWAI>2.0.CO;2.

Varin, C., N. Reid, and D. Firth, 2011: An overview of composite likelihood methods. *Stat. Sin.*, **21**, 4–42.

Wood, A. T. A., and G. Chan, 1994: Simulation of stationary Gaussian processes in $[0, 1]^d$. *J. Comput. Graphical Stat.*, **3**, 409–432, doi:10.1080/10618600.1994.10474655.